# Unconventional energetics of the pseudogap state and superconducting state in high-$T_c$ cuprates

D. N. Basov,[1] C. C. Homes,[2] E. J. Singley,[1] M. Strongin,[2] T. Timusk,[3] G. Blumberg,[4] and D. van der Marel[5]
[1]*Department of Physics, University of California, San Diego, La Jolla, California 92093-0319*
[2]*Department of Physics, Brookhaven National Laboratory, Upton, New York 11973-5000*
[3]*Department of Physics, McMaster University, Hamilton, Ontario, Canada L8S 4M1*
[4]*Bell Laboratories, Lucent Technologies, Murray Hill, New Jersey 07974*
[5]*Laboratory of Solid State Physics, University of Groningen, 9747 AG Groningen, The Netherlands*
(Received 14 March 2000; revised manuscript received 1 August 2000; published 12 March 2001)

Insight into the nature of the pairing of charge carriers in high-$T_c$ superconductors may be provided by a systematic investigation of the condensation energy. In this work we report on studies of the electronic kinetic energy across the complex phase diagram of these materials. The *c*-axis component of the electronic kinetic energy (determined from an analysis of the optical constants) is shown to be reduced below $T_c$, primarily in those compounds in which the superconducting transition at $T_c$ is preceded by the formation of the partial gap in the density of states (pseudogap) at $T^* > T_c$. An examination of the doping dependence of the infrared conductivity in conjunction with the results of photoemission spectroscopy suggests that the lowering of the kinetic energy is a property of the electronic states close to the intersection of the two-dimensional Fermi surface with the boundary of the Brillouin zone. We contrast the *c*-axis results with the energetics associated with the nodal quasiparticles probed through the in-plane conductivity.

DOI: 10.1103/PhysRevB.63.134514 PACS number(s): 74.25.Gz

## I. INTRODUCTION

After more than a decade of intensive research in high temperature superconductivity there is still no microscopic explanation for this phenomenon. The most general statement that one can make regarding the superconducting state is that the free energy of a superconductor is lowered by an amount referred to as the condensation energy $E_c$. Therefore it is natural to explore possible origins of the condensation energy in a search for the mechanism of superconductivity. An advantage of this approach is not only in its generic character, but also in the fact that the microscopic roots of the condensation energy are limited to a few basic interactions.[1] Changes of the Coulomb energy $V_C$, the electronic kinetic energy *K*, and the exchange energy *J* can be studied, at least in principle, using a variety of spectroscopies,[1–7] whereas the magnitude of $E_c$ can be extracted from the specific heat measurements.[8] According to the theory of Bardeen, Cooper, and Schrieffer (BCS), the superconducting state of elemental metals is driven by the reduction of the potential energy which overpowers the increase of the kinetic energy.[9,10] Notably, in metallic superconductors the pairing of charge carriers, the formation of the gap in the density of states, and the development of coherence between electron pairs all occur at the temperature of the superconducting transition. Numerous experiments suggest that in cuprate high-$T_c$ superconductors the above processes may take place at different temperatures[11] so that the energetics of the superconducting state is expected to be more complex. The goal of this work is to explore the systematic trends in the behavior of the electronic kinetic energy inferred from the analysis of the optical constants in different regions of the complicated phase diagram of high-$T_c$ cuprates.

## II. PROBING ELECTRONIC KINETIC ENERGY WITH INFRARED

A variety of models for the electromagnetic response of a solid allows one to derive a relationship between the integral of the real part of the complex conductivity $\tilde{\sigma}(\omega)=\sigma_1(\omega)+i\sigma_2(\omega)$ in the polarization **r** and the electronic kinetic energy $K_{\mathbf{r}}$ along this direction:[2,4,12]

$$\int_0^W d\omega\, \sigma_{1,\mathbf{r}}(\omega) = -\frac{\pi e^2 a_{\mathbf{r}}^2}{2\hbar^2} K_{\mathbf{r}}, \tag{1}$$

where $a_{\mathbf{r}}$ is the lattice spacing in the direction **r**. This equation offers an interpretation of such a well-defined experimental parameter as the effective spectral weight $N_{\mathrm{eff}}(\omega)=\int_0^{\omega} d\omega' \sigma_1(\omega')$ (middle panel in Fig. 1) in terms of the electronic kinetic energy.[13] It is therefore important to explore the consequences of this approach when it is applied to the analysis of the electromagnetic response at the boundaries of phase transitions in solids while keeping in mind possible caveats connected with the derivation of Eq. (1).

To proceed with the analysis of the kinetic energy in high-$T_c$ cuprates we first note that the superconducting state conductivity $\sigma_{1,\mathbf{r}}^{SC}(\omega)$ for any polarization **r** has two distinct contributions

$$\sigma_{1,\mathbf{r}}^{\mathrm{SC}}(\omega) = \rho_{s,\mathbf{r}}\delta(0) + \sigma_{1,\mathbf{r}}^{\mathrm{reg}}(\omega). \tag{2}$$

The first component is associated with the $\delta$ function at $\omega=0$ due to the superconducting condensate with the spectral weight given by $\rho_{s,\mathbf{r}}=\pi e^2 n_s/2m_{\mathbf{r}}^*$, where $n_s$ is the density of superconducting electrons and $m_{\mathbf{r}}^*$ is the corresponding component of their effective mass tensor. The second contribution $\sigma_{1,\mathbf{r}}^{\mathrm{reg}}(\omega)$ (usually referred to as the ''regular'' component) is defined at $\omega>0$ and is associated with the response

 

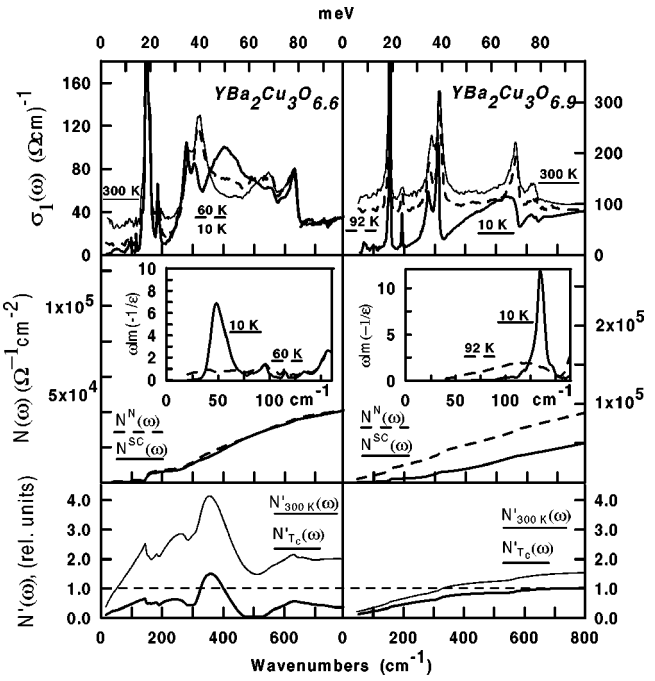


FIG. 1. Interplane response of $YBa_2Cu_3O_{6.6}$ and $YBa_2Cu_3O_{6.9}$ single crystals. Top panels: the interlayer conductivity $\sigma_1(\omega)$; middle panels: spectral weight $N(\omega)$; bottom panels: normalized spectral weight $N'(\omega)$ as defined in the text. The insets: the spectra of the first moment of the loss function. In all panels thin solid lines refer to the 300 K data; dashed lines to data at $T \simeq T_c$; and thick solid lines to data at $T=10$ K. The key difference between the two samples is the energy scale from which the superconducting condensate is collected. In the nearly optimally doped $YBa_2Cu_3O_{6.9}$ crystal with $T_c=91$ K the Ferrel-Glover-Tinkham sum rule is exhausted at $\omega < 8\ kT_c$ as indicated by (i) $N'_{T_c} \rightarrow 1$ at $\omega \simeq 600$ cm$^{-1}$ and (ii) agreement between the area confined under $\omega \times \mathrm{Im}(-1/\tilde{\epsilon})$ above and below $T_c$. In the underdoped sample the energy range of $>25\ kT_c$ produces only 40% of the condensate density as evidenced by (i) $N'_{T_c} \rightarrow 0.4$ at $\omega \simeq 800$ cm$^{-1}$ and (ii) difference by the factor of $\simeq 2$ between the area confined under $\omega \times \mathrm{Im}(-1/\tilde{\epsilon})$ above and below $T_c$. The behavior of underdoped crystals can be interpreted in terms of kinetic energy change.

of unpaired charge carriers. Combined together Eqs. (1) and (2) yield the Hirsch kinetic energy sum rule[2]

$$\rho_{s,\mathbf{r}} = \int_{0+}^{W} d\omega [\sigma_{1,\mathbf{r}}^{N}(\omega) - \sigma_{1,\mathbf{r}}^{\mathrm{SC}}(\omega)] + \Delta K_{\mathbf{r}}, \qquad (3)$$

where $N$ refers to the normal state and $\Delta K_{\mathbf{r}}$ is the change of the kinetic energy associated with the motion along direction $\mathbf{r}$. In conventional superconductors $\Delta K$ is negligibly small and the Ferrel, Glover, and Tinkham (FGT) sum rule $\rho_s = \int_{0+}^{W} d\omega [\sigma_1^N(\omega) - \sigma_1^{\mathrm{SC}}(\omega)]$ is obeyed. The FGT equation is routinely used to estimate the superfluid density in superconductors and implies that the entire ''missing area'' in the conductivity spectra $\int_{0+}^{W} d\omega [\sigma_1^N(\omega) - \sigma_1^{\mathrm{SC}}(\omega)]$ reappears in the superconducting $\delta(0)$ function. Because the superfluid density can be obtained from the imaginary part of the conductivity $\rho_s = \pi\omega\sigma_2(\omega \rightarrow 0)$ and therefore can be determined independently of the integral $\int_{0+}^{W} d\omega [\sigma_1^N(\omega) - \sigma_1^S(\omega)]$ one can evaluate changes of the kinetic energy upon superconducting transition from Eq. (3). The form of the Eq. (3) suggests that it is useful to define the normalized spectral weight $N'(\omega) = [N^N(\omega) - N^{\mathrm{SC}}(\omega)]/\rho_s$, where $N^N(\omega) = (120/\pi)\int_{0+}^{\omega} d\omega' \sigma_1^N(\omega)$ and $N^{\mathrm{SC}}(\omega) = (120/\pi)\int_{0+}^{\omega} d\omega' \sigma_1^{\mathrm{SC}}(\omega)$.[5] In conventional superconductors $N'(\omega)$ saturates at $\omega \approx 10-15\ kT_c$ reaching the level of $N' \simeq 1$.[5] According to Eq. (3) if in the saturated region $N'(\omega) \neq 1$, then this deviation from unity can be interpreted in terms of kinetic energy change.

In a previous publication[5] we reported on a significant discrepancy between $\rho_{s,c}$ and $\int_{0+}^{W} d\omega [\sigma_{1,c}^N(\omega) - \sigma_{1,c}^{\mathrm{SC}}(\omega)]$ measured in the polarization perpendicular to the $CuO_2$ layers, suggesting that the *c*-axis component of kinetic energy is lowered in certain cuprates at $T < T_c$. In this work we explore the complex phase diagram of high-$T_c$ materials from the viewpoint of the kinetic energy and show that this anomalous effect is intimately connected with the incoherent nature of the interlayer response found primarily in underdoped cuprates.[14] We employ the sum rules described above and an additional sum rule for the loss function Im $[-1/\tilde{\epsilon}(\omega)]$ which proves the consistency of our analysis. We show that the partial gap (pseudogap) developing in the density of states of $La_{2-x}Sr_xCuO_4$ (La214) and $YBa_2Cu_3O_x$ (YBCO) materials at temperature $T^* > T_c$ (Ref. 11) is in fact responsible for the anomalies of the kinetic energy seen in these compounds. Therefore, our new results have implications both for the microscopic understanding of the superconducting state, and of the pseudogap state in cuprates.

## III. EXPERIMENTAL RESULTS AND ANALYSIS OF UNCERTAINTIES

In the top panel of Fig. 1 we plot the real part of the interplane *c*-axis conductivity $\sigma_{1,c}(\omega)$ for a strongly underdoped YBCO crystal with $x=6.6$, $T_c=59$ K and for a nearly optimally doped sample with $x=6.9$, $T_c=91$ K. The *c*-axis component of the optical conductivity was obtained from the reflectance measurements using Kramers-Kronig (KK) analysis.[15] One generic feature of the interplane conductivity of most cuprates is a flat incoherent background extending over the energy scale up to a few eV.[16] The signature of the underdoped YBCO materials is a well-defined threshold structure at $\omega \simeq 300$ cm$^{-1}$ seen already at $T > T_c$.[17] In the far-infrared sharp phonon peaks are superimposed on this incoherent electronic contribution. The absolute value of $\sigma_{1,c}(\omega)$ associated with the electronic background increases from underdoped to overdoped materials. In the overdoped crystals the Drude-like behavior can be clearly identified in the spectra of $\sigma_{1,c}(\omega)$.[18] These tendencies are common for YBCO, La214, and $Tl_2Ba_2CuO_6+x$ (Tl2201) compounds[19–21] and suggest that the increase of the doping level leads to the development of coherence in the interlayer response.

The behavior of the normalized spectral weight exposes several other trends of the doping dependence of the *c*-axis charge dynamics in the YBCO series. In order to illuminate the differences between underdoped and optimally doped

crystals from the point of view of the FGT sum rule we define $N'_{T_c}(\omega)=[N^N(\omega,T\simeq T_c)-N^{\rm SC}(\omega,T\ll T_c)]/\rho_s$ (bottom panels in Fig. 1). In the $YBa_2Cu_3O_{6.9}$ crystal, the $N'_{T_c}(\omega)$ saturates at approximately $500-600$ cm$^{-1}$ reaching the value of $\simeq 1$. Therefore in this crystal the FGT sum rule is exhausted over the range $\simeq<8\ kT_c$. On the contrary, in the underdoped sample the $N'_{T_c}(\omega)$ spectrum reaches the level of only 40% at 150 cm$^{-1}$ and does not show significant variation up to 800 cm$^{-1}$ (disregarding the structure due to the temperature dependence of the phonon modes). Thus in the underdoped crystal the superfluid density significantly exceeds the ''missing area'' in the real part of the conductivity despite the fact that the integration extends to $\simeq 25kT_c$. Therefore, in accord with Eq. (3), the latter result can be interpreted in terms of the change in the *c*-axis component of the kinetic energy.

It is imperative to discuss the validity of the above results. To generate the $N'(\omega)$ spectra we extended the $\sigma_1(\omega)$ curves with a constant to $\omega=0$ below the cutoff of our measurements ($\omega\simeq 30-35$ cm$^{-1}$), a behavior that is suggested by the overall shape of the conductivity which is frequency independent at low energies. The above assumption, as well as the impact of extrapolations required for KK analysis, can be examined through the formalism of the energy loss function $\mathrm{Im}(-1/\tilde{\epsilon})$. In a conducting material the loss function shows a peak centered at $\omega$ which is proportional to the plasma frequency of charge carriers $\omega_p^2=4\pi ne^2/m^*$. It follows from Eq. (2) that in a superconductor $\omega_p^2=8\rho_s+N^{\rm SC}$. The first moment of $\mathrm{Im}(-1/\tilde{\epsilon})$ follows the sum rule

$$\int_0^\infty \omega\,\mathrm{Im}\left[-\frac{1}{\tilde{\epsilon}(\omega)}\right]d\omega=\frac{1}{2}\pi\omega_p^2. \tag{4}$$

Although Eq. (4) is equivalent to the oscillator strength sum rule for the conductivity, the advantage of the loss function formalism is that the spectra of $\mathrm{Im}(-1/\tilde{\epsilon})$ have *vanishing* weight in the extrapolated region ($\omega<35$ cm$^{-1}$). The inset in Fig. 1 shows $\omega\times\mathrm{Im}(-1/\tilde{\epsilon})$ spectra above and below $T_c$. At $T>T_c$ the plasmon feature is overdamped but at $T\ll T_c$ the sharp resonances are found in both materials. These resonances are located in the energy range which is not influenced by uncertainties of the KK procedure. The area confined under $\omega\times\mathrm{Im}(-1/\tilde{\epsilon})$ remains essentially *constant* in the $YBa_2Cu_3O_{6.9}$ crystal as the temperature is lowered from $T\simeq T_c$ down to 10 K. This is consistent with $N'_{T_c}\simeq 1$ for $\omega>0.09$ eV inferred from the conductivity sum rules. In the case of $YBa_2Cu_3O_{6.6}$ sample, the integrals of $\omega\times\mathrm{Im}(-1/\tilde{\epsilon})$ taken at $T=10$ K and at $T\simeq T_c$ differ approximately by a factor of 2 in accord with the behavior of $N'_{T_c}$ for this crystal. Thus, the loss function formalism [Eq. (4)] provides an independent corroboration of the results obtained from the conductivity spectra.

There is yet another source of uncertainty in the spectra of the normalized spectral weight. This latter source is related to possible mixing of the in-plane reflectance $R_{ab}(\omega)$ with the c-axis reflectance $R_c(\omega)$. Such mixing may result from

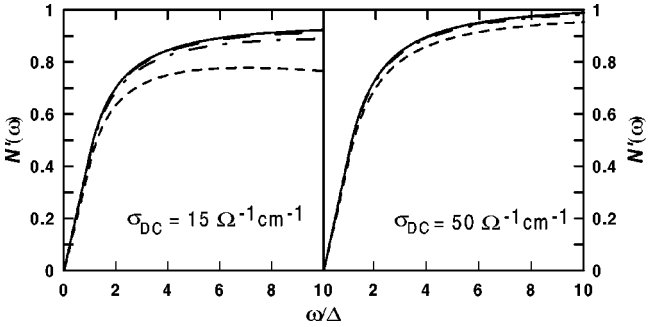


FIG. 2. Mixture between *c*-axis and *ab*-plane reflectance $R(\omega)=(1-z)R_c+zR_{ab}$ may lead to considerable deviation of the normalized spectral $N'(\omega)$ from unity. Calculations were performed as described in the text for different values of *z*: $z=0$ (solid lines), $z=0.0025$ (long dashed lines), $z=0.01$ (dash dotted line), and $z=0.05$ (short dashed line).

(i) imperfections of the polarizer, (ii) misalignment of the polarizers, and/or (iii) misorientations of single crystals if mosaic samples are used for experiments. Results shown in Fig. 1 were obtained for separate relatively large single crystals ($2000\times 250\ \mu$m$^2$) and therefore (iii) is not relevant. The specified extinction coefficient of our polarizers is better than $10^{-3}$ in the frequency range 20–1000 cm$^{-1}$. We measured somewhat larger transmission through two crossed polarizers: 0.3% at 420 cm$^{-1}$. Similar leakage of unwanted polarization can occur if a polarizer is misoriented by $\simeq 5°$. In our experiments the accuracy of the polarizer alignment is better than 2° and minor discrepancy with the specified characteristic most likely results from damage of the surface of the polarizers.

In Fig. 2 we show the impact of unwanted leakage for the spectra of $N'(\omega)$. We calculated $R(\omega)=(1-z)R_c+zR_{ab}$ for various values of *x*. To produce $R_c$ in the normal state we used $\sigma_{1,c}^N(\omega)=\sigma_{DC,c}=15$ $[\Omega\,\mathrm{cm}]^{-1}$ (left panel) and 50 $[\Omega\,\mathrm{cm}]^{-1}$ (right panel). The in-plane reflectance was calculated using the Drude model with $\omega_{p,ab}=9000$ cm$^{-1}$ and $1/\tau_{ab}=600$ cm$^{-1}$. For simplicity, we assumed isotropic *s*-wave gap at $T<T_c$ both for the in-plane and the interplane data. We then obtained the complex conductivity from the KK transformation of $R(\omega)$ followed by exactly the same analysis which we used to generate $N'(\omega)$ from the experimental data in Fig. 1. For $z=0$ (solid line) the sum rule is nearly exhausted at $10\Delta$ as expected from the FGT sum rule. The spectra for $z=0.0025$, and $z=0.01$ systematically deviate from the $z=0$ spectrum and reveal saturation at $N'<1$. The latter effect originates primarily from changes of $\sigma_1^{\rm SC}(\omega)$. The absolute value of $\rho_s$ [extracted from $\sigma_2(\omega)$] as well as the normal state conductivity are nearly unaffected by the leakage. The effect is suppressed with the increase of $\sigma_{\rm dc}$.

The spectra for $z=0.0025$ accounts for the experimental conditions of our measurements reported in this work. This value is close to the impact of the imperfection of our polarizer (based on the transmission of crossed polarizer) or to the effect produced by misalignment of the polarizer by 5°. We also note that $z=0.0025$ leakage yields less than 1% correc-

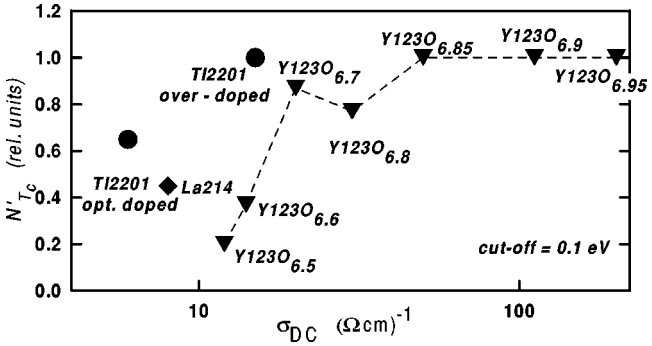


FIG. 3. Normalized spectral weight $N'_{T_c}$ obtained from the integration of the interlayer conductivity up to the cut-off energy 0.1 eV. The $N'_{T_c}$(0.1 eV) data for a variety of high-$T_c$ cuprates is plotted as a function of the dc conductivity along the *c* axis at $T \simeq T_c$. For relatively well-conductive crystals $N'_{T_c} \simeq 1$ suggesting that the FGT sum rule is exhausted at $\omega < 0.1$ eV. Deviation of $N'_{T_c}$ from unity can be interpreted in terms of the kinetic energy change. This effect is most prominent in less conductive samples. With the exception of the optimally doped $Tl_2Ba_2CuO_6$ all samples with $N'_{T_c} < 1$ show ''semiconducting'' upturn in the temperature dependence of the dc resistivity. This behavior is one of the characteristic attributes of the pseudogap state as discussed in the text.

tion of $R(\omega)$ compared to $R_c(\omega)$; such a correction is of the order of the uncertainty in the measurements of the absolute reflectance. The values of $z=0.01$ and $x=0.05$ would correspond to a misalignment of the polarization by about 10° and 20°, respectively. Such misalignment can be excluded for our experiments carried out for separate single crystals. Nevertheless, the $z=0.01$–$0.02$ situation may occur in the measurements involving mosaic samples stacked out of several single crystals.[21] While the absolute value of $\rho_s$ is still unaffected by polarization leakage effects, the spectra of $N'(\omega)$ generated for $z=0.05$ are suppressed by 10–15 % compared to the intrinsic value. In our previous work for Tl2201 mosaics, we reported $N' \simeq 0.5$ for the optimally doped crystals and $N' \simeq 0.85$ for the overdoped compound. In view of the effects of the polarization leakage discussed above, these data points were corrected by 0.15 in the results shown in Fig. 3.

We also point out that the integration of the conductivity following Eq. (1) adds the contribution due to the electronic background and due to IR-active lattice vibrations. It is known that phonons in high-$T_c$ cuprates reveal a number of nontrivial properties, including abrupt changes of the linewidth and frequency of the modes at $T < T_c$.[22,23] However, the oscillator strength of the phonon modes is usually not affected by these changes. In La214 and in Tl2201 the phonon spectrum is simpler than in YBCO series. For the former compounds we were able to subtract the phonon contribution and to perform the sum rule analysis separately for the electronic contribution.[5] This analysis confirmed that the phonon oscillator strength remains constant below $T_c$ and therefore the anomalies detected in the sum rule analysis are primarily of the electronic origin.

## IV. DISCUSSION

In Fig. 3 we present the $N'_{T_c}$ data with integration limited up to 0.1 eV for a series of $YBa_2Cu_3O_x$, $x=6.5$–$6.95$ single crystals along with the data for La214 and Tl2201 compounds.[5,21] In this diagram the $N'_{T_c}$ is plotted as a function of the dc conductivity $\sigma_{dc}$ across the layers at $T \simeq T_c$. It appears that the deviation of $N'_{T_c}$ from unity is most prominent in the materials with low dc conductivity. As $\sigma_{dc}$ increases, the magnitude of $N'_{T_c}$ is systematically enhanced and eventually reaches unity implying that the sum rule is exhausted with the relatively narrow cutoff of 0.1 eV. This trend is also similar in the YBCO, Tl2201, and La214 series.[21,26] According to Eq. (3), the magnitude of $1-N'(\omega)$ is related to kinetic energy change $\Delta K_c$. Then it follows from Fig. 3 that $\Delta K_c$ is significant only in those compounds in which the conductivity between the layers at $T > T_c$ is nearly blocked. Development of coherence in the *c*-axis response signaled: (i) by the increase of $\sigma_{dc}$ with doping, and (ii) by the formation of the Drude-like feature in the $\sigma_1(\omega)$ spectra of overdoped samples[18–21] reduces the magnitude of $\Delta K_c$. The in-plane conductivity of all materials in Fig. 3 is in the coherent regime (Drude-like) and the FGT sum rule is exhausted at $\omega < 0.1$ eV.[25] This latter result will be discussed in more details in connection with Fig. 5.

At least in YBCO and in La214 systems the changes of the *c*-axis component of the kinetic energy are clearly related to the development of the pseudogap state at $T^* > T_c$.[11] The signature of the pseudogap in the *c*-axis response of underdoped high-$T_c$ cuprates is in the transfer of the spectral weight from far-infrared to higher energies.[17] This process corresponds to suppression of $\sigma_1(\omega \rightarrow 0)$ and to characteristic ''semiconducting'' temperature dependence of the dc resistivity $\rho_{dc}$ that is commonly found in underdoped compounds. All materials in Fig. 3 for which $N'_{T_c} < 1$ show ''semiconducting'' $\rho_{dc}(T)$.[29] Thus, in the pseudogap state the charge carriers become more strongly confined to the $CuO_2$ planes while the probability of their coherent hopping across the planes is reduced. An application of Eq. (1) to the data at $T < T^*$ indicates that the kinetic energy is *enhanced* in the pseudogap state. We note that the changes of the kinetic energy both in the pseudogap state and in the superconducting state are of the same order as the magnitude of the *c*-axis kinetic energy itself. This interesting regime has to be contrasted with what typically occurs in superconducting metals.[10] In our view the fact that $\Delta K_c \simeq Kc$ is a direct consequence of the incoherent nature of the interlayer conductivity.

Further connection of the pseudogap state to the anomalies of the superfluid response can be seen from the temperature dependence of $N'(\omega)$ spectra. In order to analyze this *T* dependence we define $N'_{300\ K}(\omega) = [N^N(\omega, T=300\ \text{K}) - N^{SC}(\omega, T \ll T_c)]/\rho_{s,c}$ (thin solid lines in the bottom panels of Fig. 1) in addition to $N'_{T_C}(\omega)$ introduced earlier. The $N'_{300\ K}(\omega)$ spectrum obtained for the $YBa_2Cu_3O_{6.6}$ reaches the level of 2.2 at $\omega \simeq 150\ \text{cm}^{-1}$ indicating that there is twice as much weight in the room temperature conductivity than

what is needed to account for the superfluid density in this sample. However, as the temperature is lowered down to $T_c$ most of this spectral weight is transferred to frequencies above 0.2–0.3 eV (Refs. 15,18) so that the conductivity at $T \simeq T_c$ is strongly diminished. It is this suppression of $\sigma_{1,c}(\omega)$ in the pseudogap state that leads to nontrivial results in $N'_{T_c}(\omega)$ spectra (thick solid line). The behavior of underdoped La214 crystals is similar.[27,28] Therefore the existing data suggest that the kinetic energy change at $T<T_c$ is most conspicuous is the crystals in which superconductivity emerges out of the pseudogap state.

While the origin of the pseudogap is in dispute,[11] some experiments are consistent with the idea of pair formation taking place already at $T^*>T_c$.[30–32] The analysis of the superfluid density inferred from tera-Hertz time domain spectroscopy provides strong evidence for the preformed pairs scenario.[33] Pair formation is favored because of the decrease in the potential energy which is accompanied by inevitable increase of the kinetic energy (virial theorem). The latter result is in agreement with our data since the transfer of the spectral weight to higher energies at $T_c<T<T^*$ is indicative of the increase of $K_c$ in accord with Eq. (1). Within the preformed pair paradigm, the onset of superconductivity is associated with the phase coherence occurring at $T_c$ which is distinct from the pair formation temperature $T^*$. According to our data, the former process is associated with the partial recovery of the *c*-axis kinetic energy which was strongly enhanced in the pseudogap state. It has been argued that quantum fluctuations play an increasingly important role in the pseudogap state.[34] An account of quantum fluctuations may also lead to the deviation from the FGT sum rule with $N'_{T_c}=0.5$.[34] We remark that both the pseudogap crossover and superconducting transition affect the entire background in the spectra of the interplane conductivity.

We fail to find a correlation between the magnitude of $\Delta K_c$ at $T<T_c$ and the critical temperature of the superconductors that we have studied (top panel Fig. 4). While in the Tl2201 series the largest change of kinetic energy occurs in the crystal close to optimal doping, in the YBCO compounds $\Delta K_c$ decreases with increasing $T_c$ (Fig. 4). Also, the magnitude of $\Delta K_c$ is significantly smaller than the condensation energy at least in Tl2201 and $HgBa_2CuO_{4+x}$ materials.[35,36] In part, this discrepancy can be attributed to the formidable difficulties concerned with the estimates of the *normal* state free energy from the specific heat data in the regime when superconducting fluctuations may be present at $T_c<T<T^*$.[4] It is also important to keep in mind that ideally, Eq. (3) should be applied to the normal and superconducting state data obtained *at the same temperature* $T \to 0$. This is difficult to achieve for technical reasons. Several experiments suggest that the *normal* state conductivity continues to decrease at $T<T_c$ following the ''semiconducting'' slope of $\rho_{dc}(T)$ seen already at $T>T_c$ in underdoped samples. This possibility is supported by the resistivity data in the regime when superconductivity is suppressed by a high magnetic field.[37] High-field data show that $\sigma^N_{dc,c}(T \ll T_c) < \sigma^N_{dc,c}(T \simeq T_c)$ in underdoped La214 crystals.[37] Also, careful analysis of $\sigma_{1,c}(\omega)$ in midinfrared range demonstrates that some of the spectral

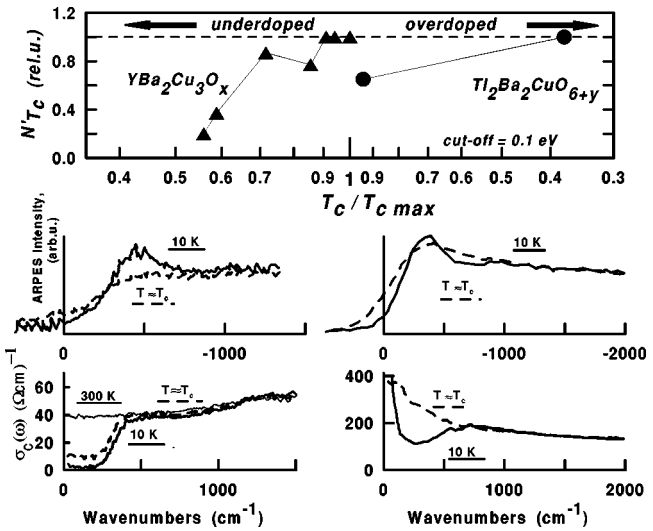


FIG. 4. Top panel: Normalized spectral weigh $N'_{T_c}$ calculated with the cutoff energy 0.1 eV plotted as a function of the ratio $T_c/T_{c\ \max}$ for a series of $YBa_2Cu_3O_x$ and $Tl_2Ba_2CuO_{6+y}$ single crystals. We fail to find a correlation between the magnitude of $N'_{T_c}$ (related to the change of the kinetic energy) and the critical temperature of studied superconductors. ARPES intensity measured for momenta close to $(\pi,0)$ for underdoped Bi2212 crystal (Ref. 44) (left middle panel) and for overdoped Bi2212 sample (Ref. 46) (right middle panel). Dashed lines: at $T \simeq T_c$; solid lines at $T=10$ K. Infrared *c*-axis conductivity for underdoped $YBa_2Cu_3O_{6.7}$ crystal (left bottom panel) and for overdoped $YBa_2Cu_3O_7$ sample (Ref. 17) (right bottom panel). Only the electronic background is shown; the phonon absorption has been subtracted by fitting to oscillators. Both ARPES and IR results indicate that underdoped samples show lowering of the kinetic energy at $T<T_c$ (as described in the text). The normal state properties in the underdoped regime are markedly different from conventional Fermi-liquid behavior. In the overdoped crystal the kinetic energy is unchanged below the temperature of superconducting transition. Crystals on the overdoped side of the phase diagram reveal more conventional normal state behavior: quasiparticle peak in the ARPES spectra as well as the Drude-like feature in $\sigma_{1,c}$ can be resolved already at $T>T_c$.

weight missing from the conductivity at $T<T_c$ is transferred to high energies and not to the $\delta$ function even in the optimally doped single crystals.[18,38] Thus, it is conceivable that $\sigma^N_{1,c}(\omega, T \ll T_c) < \sigma^N_{1,c}(\omega, T \simeq T_c)$, and that the integral term in Eq. (3) may be *vanishingly small* throughout the range of infrared frequencies. Then the actual changes of $\Delta K_c$ may be as large as $\rho_s$.

Suppression of the *c*-axis kinetic energy at $T<T_c$ is consistent with a recent analysis of the angular resolved photoemission (ARPES) data for $Bi_2Sr_2CaCu_2O_{8+x}$ (Bi2212). Norman *et al.* proposed the so-called mode model which successfully describes many important attributes of the photoemission experiments.[7] An important feature of this model is that it suggests lowering of the kinetic energy associated with the formation of the quasiparticle peak in the ARPES spectra. The comparison of interlayer infrared (IR) results and of the ARPES data is facilitated by the peculiarity of the *c*-axis tunneling matrix elements which are maximized for the momenta parallel to $(\pi,0)$ or $(0,\pi)$ and vanish along

the nodal $(\pi,\pi)$ direction.[39,34,40] This conjecture is supported by a clear connection between the pseudogap features detected in the *c*-axis conductivity and ARPES spectra measured close to the $(\pi,0)$.[41–43] Further parallels between the information extracted from these two techniques can be revealed in the context of the energetics of the superconducting state. Numerous photoemission experiments show that the spectral function $A[\omega,(\pi,0)]$ at $T>T_c$ is very broad with only small weight near the Fermi energy $E_F$.[44,45] However, below $T_c$ a well-defined quasiparticle peak (QP) emerges (Fig. 4) suggesting that the momentum distribution function $\nu(k)$ (Ref. 50) sharpens below the transition temperature. Since the electronic kinetic energy is minimized if $\nu(k)$ has a sharp step at $E_F$,[9] the latter result is in accord with the reduction of $K$ at $T<T_c$. These changes in the ARPES spectra in the superconducting state are most prominent in the underdoped samples. With increasing doping, the QP peak in the ARPES spectra becomes visible already in the normal state.[46,47] The presence of this peak in the spectra obtained for optimally and overdoped crystals precludes significant lowering of the kinetic energy in these samples at $T<T_c$. Therefore, the doping dependence of $\Delta K$ suggested by the ARPES experiments fits the pattern inferred from the analysis of the *c*-axis conductivity summarized in Fig. 3.

The key outcome of both IR and ARPES experiments is that the kinetic energy change is found exclusively in the materials for which the normal state properties are marked by a strong degree of incoherence and are therefore distinct from the conventional Fermi-liquid picture. A broad and structureless ARPES spectral function can be viewed as an obvious sign of non-Fermi-liquid ground state.[51] The corresponding hallmark in the spectra of $\sigma_{1,c}(\omega)$ is a flat background. The kinetic energy is lowered upon the superconducting transition *only* if the above features can be distinguished in the normal state response (left panels in Fig. 4). Both of these characteristics of the underdoped regime fade away as the doping progresses towards the overdoped side of the phase diagram. Indeed, overdoped crystals show a well-defined QP peak in the ARPES spectra consistent with the Drude-like behavior of $\sigma_{1,c}(\omega)$ (right panels of Fig. 4). The magnitude of the kinetic energy change is reduced and eventually vanishes in overdoped regime. Thus it appears that the lowering of the kinetic energy is an attribute of the transition to the coherent state at $T<T_c$ provided the coherence is lacking above $T_c$. The formation of the pseudogap ''enhances'' the non-Fermi-liquid character of both the interlayer conductivity and of the ARPES spectra by shifting the spectral weight to higher energies. In this way the pseudogap state is beneficial for the observation of the kinetic energy change. A comparison of IR and ARPES results indicates that the lowering of the kinetic energy is not related to the interplane transport *per se* but rather reflects the property of the electronic states close to the boundary of the Brillouin zone at $(\pi,0)$ and $(0,\pi)$ points.

The analysis of the in-plane conductivity may provide an insight into the superconducting state energetics close to the nodal $(\pi,\pi)$ direction. Despite the fact that $\sigma_{ab}(\omega)$ is averaged over the entire Fermi surface, the regions close to $(\pi,0)$ and $(0,\pi)$ give only a minor contribution because the Fermi velocity in these regions is (vanishingly) small. Therefore, the segments of the Fermi surface close to the node of the *d*-wave gap at $(\pi,\pi)$ dominate in the *ab*-plane transport. The results of the sum rule analysis of the *a*-axis conductivity for $YBa_2Cu_3O_{6.6}$ (Ref. 24) and of the *ab*-plane conductivity for the optimally doped $Tl_2Ba_2CuO_{6+y}$ (Ref. 48), are shown in Fig. 5. Here we plot the difference between the spectral weight at $T_c$ and at 10 K $[N^N(\omega)-N^{SC}(\omega)]$ without normalizing the spectra by the magnitude of the superfluid density. The absolute values of $\rho_s$ (determined from the imaginary conductivity) are shown with the dashed lines. The *a*-axis data reveal a reasonable agreement between the

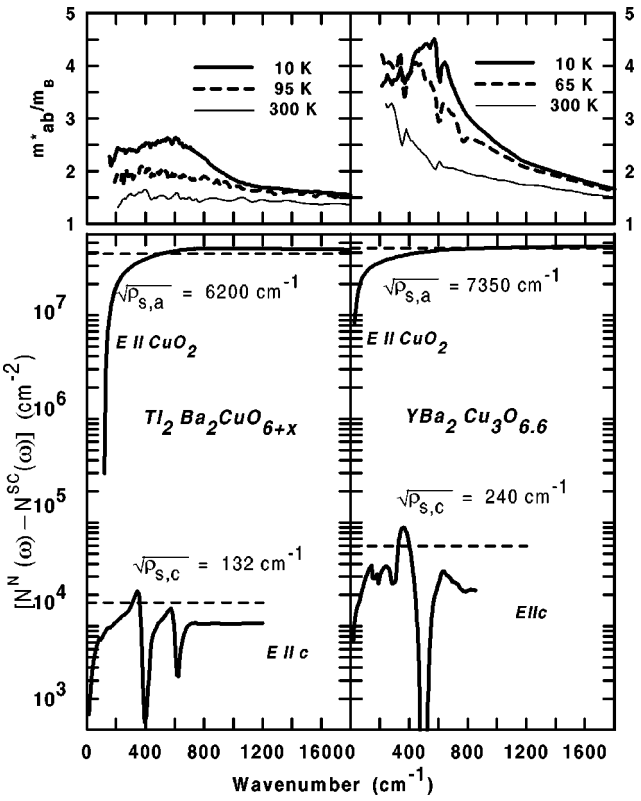


FIG. 5. Lower panels: the spectra of $[N^N(\omega,T\simeq T_c)-N^{SC}(\omega)]$ reveal the sum rule result for the superfluid density in the optimally doped $Tl_2Ba_2CuO_{6+y}$ (left) and $YBa_2Cu_3O_{6.6}$ (right) single crystals. The dashed line show the magnitude of $\rho_s$ extracted from the imaginary part of the conductivity. In the case of the *c*-axis response we find the discrepancy between $[N^N(\omega,T\simeq T_c)-N^{SC}(\omega)]$ in the saturated region and the magnitude of $\rho_s$ which can be interpreted here in terms of the lowering of the *c*-axis kinetic energy at $T<T_c$. In the case of the response of the $CuO_2$ planes we find a better agreement between the two approaches to quantify the strength of the superconducting condensate. The crossing of the $[N^N(\omega,T\simeq T_c)-N^{SC}(\omega)]$ spectra measured for the *ab*-plane with the dashed lines signal some increase of the in-plane kinetic energy below $T_c$. The effect is small and comparable to the error bars in the *ab*-plane measurements. Upper panels: the spectra of the energy depended effective mass $m^*$ normalized by the magnitude of the band mass $m_B$ determined from Eq. (5) for $Tl_2Ba_2CuO_{6+y}$ (left) and $YBa_2Cu_3O_{6.6}$ (right) single crystals. Strong enhancement of effective mass at 10 K is indicative of an increase of the in-plane kinetic energy.

density of the condensate extracted from the sum rule and from the imaginary conductivity. After a closer inspection one can notice crossing between the $[N^N(\omega)-N^{SC}(\omega)]$ spectra and the dashed lines quantifying the strength of the in-plane condensate. This latter effect may signal some increase of the in-plane kinetic energy below $T_c$ that can be contrasted with the *c*-axis behavior. The effect is rather small and comparable to the error bars in the *ab*-plane measurements. However, even minor discrepancy between the two results may lead to a huge absolute value of $\Delta K_{ab}$ because the in-plane superfluid density is dramatically enhanced compared to the $\rho_{s,c}$.

Additional information on the in-plane energetics can be inferred from the analysis of the *a*-axis response in terms of the extended Drude model. This analysis allows one to obtain the energy dependence of the electronic effective mass $m^*(\omega)$ (Ref. 49):

$$\frac{m^*(\omega)}{m_B}=\frac{\omega_p^2}{4\pi}\frac{\sigma_2(\omega)}{\sigma_1^2(\omega)+\sigma_2^2(\omega)}\frac{1}{\omega}, \tag{5}$$

where $m_B$ is the band mass and $\omega_p$ is the plasma frequency obtained from the integration of the conductivity up to 1.2 eV. Within the tight-binding approximation the electronic kinetic energy is proportional to $-1/m^*$. The spectra of $m^*/m_B$ for the optimally doped $Tl_2Ba_2CuO_{6+y}$ and $YBa_2Cu_3O_{6.6}$ are shown in the top panel of Fig. 5. The mass enhancement is strongest at the lowest energies whereas at $\omega>2000$ cm$^{-1}$ the magnitude of $m^*$ is approaching the band mass. For both systems the spectra of $m^*(\omega)$ obtained at 10 K are nonmonotonic suggesting coupling of the conducting carriers to a mode at $\omega\simeq 500$ cm$^{-1}$.[49] In both crystals we find an increase of the effective mass at 10 K compared to the data at $T\simeq T_c$. This result is in accord with the increase of the in-plane kinetic energy suggested by the sum rule data in the lower panel. The fact that the in-plane and interplane results suggests different energetics at $T<T_c$ is not entirely surprising since these two measurements probe the different regions of the Fermi surface. Previous (magneto)transport studies and ARPES experiments revealed differences in the character of the electronic states at $(\pi,0)$ and in the nodal region.[52,53]

## V. CONCLUSIONS

We show that a variety of cuprates reveal changes of the *c*-axis electronic kinetic energy. The effect is intimately connected with the development of the pseudogap state and is therefore most conspicuous in underdoped materials. The *c*-axis kinetic energy is enhanced in the pseudogap state consistent with the idea of preformed pairs. In the superconducting state this enhancement is partially recovered. With the development of coherence in the *c*-axis transport, changes of the kinetic energy are suppressed and completely disappear in the overdoped materials. Within the assumption that the interlayer conductivity probes the electronic states close to the boundary of the Brillouin zone we can conclude that the effects observed in the *c*-axis transport reflect the situation close to $(\pi,0)$ and $(0,\pi)$ points. On the contrary, the in-plane conductivity is dominated by the nodal $(\pi,\pi)$ direction and reveal more conventional energetics (increase of $K_{ab}$). The contrasting behavior seen in the *c*-axis and *a*-axis data may reflect the radical distinctions between the electronic states close to the boundary of the Brillouin zone compared to the nodal direction. Both this result as well as the trends in the doping dependence seen in ARPES and IR data clearly show that the kinetic energy lowering is inherently connected with an incoherent normal state response. Possible connections between incoherent normal state response and changes of kinetic energy below $T_c$ were recently discussed in several publications.[54,55]

## ACKNOWLEDGMENTS

The authors acknowledge numerous discussions with J.E. Hirsch, S. Chakravarty, P.W. Anderson, J.P. Carbotte, R.C. Dynes, V.J. Emery, M. Imada, P.D. Johnson, A.J. Millis, M.R. Norman, P.M. Platzman, and S. Tajima. This work was supported by the NSF and U.S. DOE.

[1] A.J. Leggett, J. Phys. Chem. Solids **59**, 1729 (1998).

[2] J.E. Hirsch, Physica C **199**, 305 (1992); J.E. Hirsch and F. Marsiglio, *ibid.* (to be published).

[3] P.W. Anderson, *The Theory of Superconductivity in the High-$T_c$ Cuprates* (Princeton University Press, Princeton, 1998); Science **279**, 1196 (1998).

[4] S. Chakravarty, Eur. Phys. J. B **5**, 337 (1998); S. Chakravarty, H.-Y. Kee, and E. Abrahams, Phys. Rev. Lett. **82**, 2366 (1999).

[5] D.N. Basov, S.I. Woods, A.S. Katz, E.J. Singley, R.C. Dynes, M. Xu, D.G. Hinks, C.C. Homes, and M. Strongin, Science **283**, 49 (1999).

[6] D.J. Scalapino and S.R. White, cond-mat/9805075 (unpublished); E. Demler, and S.-C. Zhang, Nature (London) **396**, 733 (1998); P.Dai *et al.* (unpublished).

[7] M.R. Norman, M. Randeria, B. Janko, and J.C. Campuzano, Phys. Rev. B **61**, 14 742 (2000).

[8] K. Ghiron, M.B. Salamon, B.W. Veal, A.P. Paulikas, and J.W. Downey, Phys. Rev. B **46**, 5837 (1992); J.W. Loram, K.A. Mirza, J.R. Cooper, W.Y. Liang, and J. Wade, J. Supercond. **7**, 243 (1994). Note that determination of the magnitude of $E_c$ from the specific heat measurements is nontrivial if the superconducting fluctuations are present already in the normal state (Ref. 4).

[9] J.R. Schrieffer, *Theory of Superconductivity* (Benjamin, New York, 1971).

[10] In metallic superconductors potential energy and kinetic energy are both large and are almost equal in magnitude. The fractional changes of both energies at $T<T_c$ is small and to the best of our knowledge has not been investigated spectroscopically. We will show below that in the case of the *c*-axis conductivity of high-$T_c$ cuprates changes of the kinetic energy are of same order of magnitude as the kinetic energy itself. We also checked, that

parameters representative for the density of states and the gap of high-$T_c$ cuprates give a reduction of the potential energy, an increase of the kinetic energy, and a condensation energy all of the same order of magnitude.

[11] For a recent review see T. Timusk and B. Statt, Rep. Prog. Phys. **62**, 61 (1999), and references therein.

[12] P.F. Maldague, Phys. Rev. B **16**, 2437 (1977); B.S. Shastry and B. Sutherland, Phys. Rev. Lett. **65**, 243 (1990); M.V. Klein and G. Blumberg, Science **283**, 42 (1999); E.H. Kim, Phys. Rev. B **58**, 2452 (1998).

[13] Generally, the cutoff energy $W$ in Eq. (1) is of the order of the band width.

[14] The terms ''underdoped'' and ''overdoped'' usually refer to the doping regimes when the critical temperature is reduced from the maximum (optimal) value by reducing or increasing the carrier density.

[15] C.C. Homes, T. Timusk, R. Liang, D.A. Bonn, and W.N. Hardy, Physica C **254**, 265 (1995).

[16] S.L. Cooper and K.E. Gray, in *Physical Properties of High-Temperature Superconductors IV*, edited by D.M. Ginsberg (World Scientific, Singapore, 1994).

[17] C.C. Homes, T. Timusk, R. Liang, D.A. Bonn, and W.N. Hardy, Phys. Rev. Lett. **71**, 1645 (1993); D.N. Basov, T. Timusk, B. Dabrowski, and J.D. Jorgensen, Phys. Rev. B **50**, 3511 (1994).

[18] J. Schützmann, S. Tajima, S. Miyamoto, and S. Tanaka, Phys. Rev. Lett. **73**, 174 (1994); S. Tajima, J. Schtzmann, S. Miyamoto, I. Terasaki, Y. Sato, and R. Hauff, Phys. Rev. B **55**, 6051 (1997).

[19] S. Uchida, K. Tamasaku, and S. Tajima, Phys. Rev. B **53**, 1 (1996).

[20] C.C. Homes, S. Kamal, D. Bonn, R. Liang, W.N. Hardy, and B.P. Clayman, Physica C **296**, 230 (1998).

[21] A.S. Katz, S.I. Woods, E.J. Singley, T.W. Li, M. Xu, D.G. Hinks, R.C. Dynes, and D.N. Basov, Phys. Rev. B **61**, 5930 (2000).

[22] A. Litvinchuk, C. Thomsen, and M. Cardona, in *Physical Properties of High-$T_c$ Superconductors*, edited by D. Ginsberg (World Scientific, Singapore, 1994j).

[23] H. Mook, M. Mostoller, J.A. Harvey, N.W. Hill, B.C. Chakoumakos, and B.C. Sales, Phys. Rev. Lett. **65**, 2712 (1990).

[24] D.N. Basov, R. Liang, B. Dabrowski, D.A. Bonn, W.N. Hardy, and T. Timusk, Phys. Rev. Lett. **77**, 4090 (1996).

[25] L.D. Rotter *et al.*, Phys. Rev. Lett. **67**, 2741 (1990); D.N. Basov, R. Liang, D.A. Bonn, W.N. Hardy, B. Dabrowski, M. Quijada, D.B. Tanner, J.P. Rice, D.M. Ginsberg, and T. Timusk, *ibid.* **74**, 598 (1995); D.B. Tanner *et al.*, Ferroelectrics **177**, 83 (1996).

[26] So far, kinetic energy change in La214 series has not been explored systematically. Nevertheless, the few experimental results that exist seem to support the pattern of behavior seen in YBCO and Tl2201 systems. Indeed, underdoped La214 crystal studied in Ref. 5 shows the change of the kinetic energy with $N'_{T_c}(0.1\ \mathrm{eV}) \simeq 0.38$. In the nearly optimally doped sample [J. Kim, H. Somal, M. Czyzyk, D. van der Marel, A. Wittlin, A. Gerrits, V. Duijn, N. Hien, and A.A. Menovsky, Physica C **247**, 297 (1995)] $N'_{T_c}(0.1\mathrm{eV}) \simeq 0.5$.

[27] D.N. Basov, H.A. Mook, B. Dabrowski, and T. Timusk, Phys. Rev. B **52**, R13 141 (1995).

[28] Further connection between the pseudogap state and the *c*-axis electrodynamics has been recently reported by C. Panaganapolous, J.R. Cooper, T. Xiang, Y.S. Wang, and C.W. Chu, Phys. Rev. B **61**, 3808 (2000) who found rapid increase of the *c*-axis penetration depth in the underdoped regime.

[29] Although the optimally doped Tl2201 single crystals do reveal a change in kinetic energy (Ref. 5), so far there have been no reports of a pseudogap in this series of high-$T_c$ materials based on the transport data. Surprisingly, optimally doped Tl2201 crystals show ''metallic'' $\rho_{c,\mathrm{dc}}(T)$ despite the fact that the dc conductivity is as small as $\simeq 10\ (\Omega\ \mathrm{cm})^{-1}$. One possible resolution of this puzzle may be related to the peculiarities of oxygen doping of Tl2201. Since doping is interstitial, oxygen disorder is inevitable in Tl2201 compounds. It is known that when oxygen disorder is deliberately introduced in underdoped YBCO, resistivity no longer shows ''semiconducting'' up turn but, instead, reveals a ''metallic'' slope of the $T$ dependence [J.Z. Wu, N. Yu, and W.K. Chu, Phys. Rev. B **48**, R9929 (1993)]. These experiments suggest that oxygen disorder effectively creates ''shorts'' for the *c*-axis currents that obscure the intrinsic behavior of the resistivity of YBCO, and possibly of Tl2201 as well. The impact of shorts on the optical conductivity is less important since in the optical experiments the bulk of crystal is probed.

[30] V.J. Emery and S.A. Kivelson, Nature (London) **374**, 4347 (1995).

[31] Y. Uemura, in *Proceedings of the Workshop on Polarons and Bipolarons in High-$T_c$ Superconductors and Related Materials*, edited by E.K.H. Salje (Cambridge University Press, Cambridge, 1995), p. 453.

[32] Q. Chen, K. Levin, and I. Kosztin, cond-mat/0009450 (unpublished).

[33] J. Corson, R. Mallozzi, J. Orenstein, J.N. Eckstein, and I. Bozovic, Nature (London) **398**, 221 (1999).

[34] L.B. Ioffe and A.J. Millis, Science **285**, 1241 (1999); cond-mat/9908366 (unpublished).

[35] D. van der Marel, in *Proceedings of the 10-th Anniversary HTS workshop on Physics, Material and Applications* (World Scientific, Singapore, 1996), p. 357; J. Schutzmann *et al.*, Phys. Rev. B **55**, 11 118 (1997); K.A. Moler, John R. Kirtley, D.G. Hinks, T.W. Li, and Ming Xu, Science **279**, 1193 (1998); A.A. Tsvetkov *et al.*, Nature (London) **395**, 360 (1998).

[36] J. Kirtley, K.A. Moler, G. Villard, and A. Maignan, Phys. Rev. Lett. **81**, 2140 (1998).

[37] G.S. Boebinger *et al.*, Phys. Rev. Lett. **77**, 5417 (1996).

[38] M. Grnuninger, D. van der Marel, A.A. Tsvetkov, and A. Erb, Phys. Rev. Lett. **84**, 1575 (2000); D. Munzar, C. Bernhard, A. Golnik, J. Humlicek, and M. Cardona, Solid State Commun. **112**, 365 (1999); C. Bernhard, D. Munzar, A. Golnik, C.T. Lin, A. Wittlin, J. Humlmek, and M. Cardona, Phys. Rev. B **61**, 618 (2000).

[39] S. Chakravarty, A. Sudbo, P.W. Andersen, and S. Strong, Science **261**, 337 (1993); O.K. Andersen, A.I. Liechtenstein, O. Jepsen, and F.J. Paulsen, J. Phys. Chem. Solids **56**, 1573 (1995); T. Xiang, C. Panagopoulos, and J.R. Cooper, Int. J. Mod. Phys. **12**, 1007 (1998).

[40] D. van der Marel, Phys. Rev. B **60**, R765 (1999).

[41] The argument regarding the momentum dependence of the interlayer tunneling matrix elements proposed in Ref. 39 applies to the materials with the simple tetragonal structure and is somewhat questionable for compounds like Tl2201 or Bi2212 (Ref. 40).

[42] C. Bernhard *et al.*, Phys. Rev. B **59**, 6631 (1999).

[43] It is somewhat unfortunate that we are forced to compare the ARPES and IR results obtained for two different families of high-$T_c$ cuprates. Such a comparison may be justified by the fact that the key features of the Fermi surface discussed here are related to the $CuO_2$ planes and therefore are generic for all cuprates. Bi2212 series is advantageous for the studies by means of ARPES and other surface sensitive techniques because the single crystals of these materials can be easily cleaved in ultrahigh vacuum conditions. However, the absolute value of the electronic background in the *c*-axis IR spectra is very weak and is difficult to investigate accurately.

[44] H. Ding, *et al.*, Nature (London) **382**, 51 (1996).

[45] A.G. Loeser, Z.-X. Shen, D.S. Dessau, D.S. Marshall, C.H. Park, P. Fournier, and A. Kapitulnik, Science **273**, 325 (1996).

[46] P.J. White, Z.-X. Shen, C. Kim, J.M. Harris, A.G. Loeser, P. Fournier, and A. Kapitulnik, Phys. Rev. B **54**, 15 669 (1996).

[47] A.V. Fedorov, T. Valla, P.D. Johnson, Q. Li, G.D. Gu, and N. Koshizuka, Phys. Rev. Lett. **82**, 2179 (1999).

[48] A.V. Puchkov, T. Timusk, S. Doyle, and A.M. Hermann, Phys. Rev. B **51**, 3312 (1995).

[49] A.V. Puchkov, D.N. Basov, and T. Timusk, J. Phys.: Condens. Matter **8**, 10 049 (1996).

[50] The momentum distribution function is related to the integral of the spectral function $A(\mathbf{k},\omega)$ over energy.

[51] The Fermi-liquid theory implies that quasiparticles with $E=E_F$ have infinite lifetime at $T=0$ that would correspond to $\delta$- function peak in the spectral function. At higher temperature or energies the lifetime is reduced.

[52] A. Carrington, A. Mackenzie, C. Lin, and J.R. Cooper, Phys. Rev. Lett. **69**, 2855 (1992); B. Stojkovic and D. Pines, *ibid.* **76**, 811 (1996).

[53] T. Valla *et al.*, Phys. Rev. Lett. **85**, 828 (2000).

[54] Wonkee Kim and J.P. Carbotte, Phys. Rev. B **62**, 592 (2000).

[55] M. Imada and S. Onoda, cond-mat/0008050 (unpublished).